

Array Feed Synthesis for Correction of Reflector Distortion and Vernier Beamsteering

S. J. Blank

Center for Technology
Holon, Israel

W. A. Imbriale

Radio Frequency and Microwave Subsystems Section

This article describes an algorithmic procedure for the synthesis of planar array feeds for paraboloidal reflectors to simultaneously provide electronic correction of systematic reflector surface distortions as well as a vernier electronic beamsteering capability. Simple "rules of thumb" for the optimum choice of planar array feed configuration (i.e., number and type of elements) are derived from a parametric study made using the synthesis procedure described herein. A number of f/D ratios and distortion models were examined that are typical of large paraboloidal reflectors. Numerical results are presented showing that, for the range of distortion models considered, good on-axis gain restoration can be achieved with as few as seven elements. For beamsteering to ± 1 beamwidth (BW), 19 elements are required. For arrays with either 7 or 19 elements, the results indicate that the use of high-aperture-efficiency elements (e.g., disk-on-rod and short backfire) in the array yields higher system gain than can be obtained with elements having lower aperture efficiency (e.g., open-ended waveguides). With 37 elements, excellent gain and beamsteering performance to ± 1.5 BW are obtained independent of the assumed effective aperture of the array element.

An approximate expression is derived for the focal-plane field distribution of the distorted reflector. Contour plots of the focal-plane fields are also presented for various distortion and beam scan angle cases.

The results obtained show the effectiveness of the array feed approach.

I. Introduction

This article describes an algorithmic procedure for the synthesis of planar array feeds to simultaneously provide electronic correction of paraboloidal reflector antenna distortion as well as a vernier electronic beamsteering capability. This technique would be useful for correcting the gain loss and

beam squint errors that are caused by systematic reflector distortions such as those induced by gravity on large ground station antennas. These distortions are large-scale and can be measured and/or predicted with reasonable accuracy by analytic methods. This study is not concerned with random surface errors, which are usually relatively small and must be analyzed statistically.

Rudge and Davies (Ref. 1) discussed the array feed for distortion correction and proposed the use of the Butler matrix as an ingenious means of providing adaptive excitation of the feed array. Their analytic and quantitative results, however, are limited to cylindrical reflectors having one-dimensional distortion profiles requiring only linear array feeds. Amitay and Zucker (Ref. 2) analyzed the use of planar array feeds for aberration correction in spherical reflectors. Their synthesis procedure, however, relies heavily on the circular symmetry of the feed-plane field distribution that exists in this case.

The synthesis algorithm and computer code used in this study are a modification of that developed by Imbriale et al. (Ref. 3). The code includes a numerical search routine that could be used to optimize general performance criteria including gain, sidelobe levels, and beamshape. In this article, however, only gain maximization is considered. Preliminary results showing feasibility of the technique have previously been reported by Blank and Imbriale (Ref. 4). For a given feed configuration, reflector f/D ratio, and distortion profile, the algorithm finds the optimum values of the individual feed excitations to maximize the reflector antenna gain in some desired direction. In doing this, the algorithm uses the Jacobi-Bessel technique (Ref. 5) to calculate the secondary fields of the reflector antenna having an arbitrary (i.e., distorted) shape and an illumination resulting from the displaced sources that comprise the array feed. The optimum choice of the array feed configuration (i.e., the number and type of element radiators) is determined by a parametric study made on a range of f/D ratios and reflector distortion profiles. A qualitative discussion of the choice of these feed parameters is given in the section on numerical results. Questions of system cost, signal-to-noise (S/N) ratio, and hardware availability are not explicitly considered.

It is assumed that the projected aperture of the reflector is sufficiently large (i.e., $D \geq 100\lambda$) so that the effects of feed blockage on system gain can be neglected. This study is limited to fixed planar feed arrays of identical elements located in the focal plane.

Contour plots of focal plane field distributions are presented to give graphical insight into the effects of reflector distortion. An analytic expression is also given for the focal plane field distribution based on the scalar diffraction equation. The expression is valid for small magnitudes of reflector distortion and large f/D ratios.

Cross-polarization effects are not considered in this study, although in principle, an array feed could also be used to synthesize some desired polarization distribution, by, for example, varying the orientation of the feed elements or by

employing coupling effects. The array feed approach coupled with numerical search opens up the possibility of adaptive closed-loop optimization of system performance.

II. Reflector Feed Configuration

The reflector/feed configuration addressed is the case of single reflector systems¹ having circular apertures of diameter D and maximum subtended angle $\hat{\psi}$ (Fig. 1). The feed consists of either a single circular element (taken as a reference for gain calculations) or a triangular grid array of 7, 19, or 37 elements (Fig. 2). The elements of the array are presumed to be identical and to have circularly symmetric, unidirectional radiation patterns of the form

$$f(\psi) = \cos^q(\psi) \quad (1)$$

The assumption of circularly symmetric element radiation patterns is made for the purpose of simplifying the presentation of results. The technique being described can also be used with more general types of element radiation patterns.

The minimum center-to-center spacing d_e (footnote 2), between the elements of the array, is related to q , the exponent in Eq. (1), by

$$d_e = \sqrt{\frac{q + 0.5}{b}} \quad (2)$$

where the value of b depends on the type of element used (Ref. 7). For circular waveguide elements, $b = 2.07$. For radiators with a higher effective aperture, such as disk-on-rod elements, a representative value of $b = 2.47$ is used.

For given values of b and q , spacing the elements greater than d_e would imply gain loss, since the "open" area thereby left between elements would not be available to capture incident energy. Therefore, in what follows, the element spacings are set equal to d_e , not more nor less. The maximum diameter, d_f , of such a "well-packed" array feed cluster is given by

$$d_f = K \cdot d_e \quad (3)$$

where $K = 1, 2, 3, 7$, corresponding to the number of feed elements $N = 1, 7, 19, 37$, respectively.

¹Cassegrain systems can be considered in terms of equivalent single reflector systems having the appropriate f/D ratio (Ref. 6).

²Alternatively, d_e can be considered the minimum element diameter.

III. Calculation of Gain

In what follows, the gain of the reflector antenna $G(\theta_0, \phi_0)$ is taken to be synonymous with its directivity so that

$$G(\theta_0, \phi_0) = \frac{|E(\theta_0, \phi_0)|^2}{P_T/4\pi} \quad (4)$$

where $E(\theta_0, \phi_0)$ is the value of the field of the secondary pattern at the peak of its mainlobe, and P_T , the total power radiated by the antenna as a whole, is equal to that power radiated by the feed array.

Referring to Fig. 1, we have

$$E(\theta_0, \phi_0) = \sum_{i=1}^N a_i F_i \exp [jkr_i \sin \theta_0 \cos (\phi_0 - \phi'_i)] \quad (5)$$

where

N = number of elements in the array

k = propagation constant

a_i = complex excitation of the i^{th} element in the feed array

r_i, ϕ'_i = polar coordinates of the i^{th} element in the focal plane, i.e., $x_i = r_i \cos \phi'_i$, $y_i = r_i \sin \phi'_i$ (r_i is normalized to wavelength)

F_i = complex vector field received by the i^{th} array element as a result of a plane wave incident on the reflector aperture from the direction (θ_0, ϕ_0) , and

$$P_T = \int_0^{2\pi} \int_0^{\pi/2} \left| f(\theta, \phi) \sum_{i=1}^N a_i \exp [jkr_i \sin \theta \cos (\phi - \phi'_i)] \right|^2 \times \sin \theta \, d\theta \, d\phi \quad (6)$$

where $f(\theta, \phi)$ is the field pattern of the element used in the array. (All elements are assumed to be identical and mutual coupling effects are neglected.)

By reciprocity, the $\{F_i\}$ can also be viewed as the secondary fields resulting from the illumination of the reflector by the offset elements that comprise the array feed. The $\{F_i\}$ are calculated using the Jacobi-Bessel method (Ref. 5).

The gain of the reflector is maximized in a given direction by setting the feed element excitations, $\{a_i\}$, to be the conju-

gate values of the $\{F_i\}$ fields received from that direction. In those cases where the performance criteria are other than simply maximizing gain in a given direction, or when it is not practical from a hardware point of view to take the conjugate values of the fields, then it is necessary to use a numerical search algorithm such as the Rosenbrock method (Ref. 8) to find the feed excitations that optimize performance.

The ideal maximum gain of the reflector is $(\pi D/\lambda)^2$. However, it is perhaps more meaningful to reference the gains achieved with an array feed to that obtained with a single element feed having a pattern giving, say, a -10 dB aperture taper at the maximum subtended angle $\hat{\psi}$. In this case, the value of the exponent for a single element feed, q_1 , can be found from the expression

$$\frac{(\cos \hat{\psi})^{q_1}}{(f + D^2/16f)} = 0.316 \quad (7)^3$$

which, after suitable approximations, reduces to

$$q_1 \cong 9.2 (f/D)^2 - 0.5 + \frac{1}{64 (f/D)^2} \cong 9.2 (f/D)^2 - 0.5 \text{ for } f/D \geq 1 \quad (8a)$$

Together with Eq. (2), this gives

$$d_{e1} \cong \sqrt{\frac{9.2}{b}} (f/D) \quad (8b)$$

For an arbitrary value t of desired aperture field taper,

$$q_1 \cong \frac{-8 \ln(t)}{b} (f/D)^2 - 0.5 \quad (8c)$$

which, with Eq. (2), gives

$$d_{e1} \cong \sqrt{\frac{-8 \ln(t)}{b}} (f/D) \quad (8d)$$

IV. The Algorithmic Procedure

The method being described here can be used to optimize general performance criteria such as gain, sidelobe levels, and beamshape. In this study, however, only gain maximization

³ $\hat{\psi} = 2 \tan^{-1} (1/4f/D)$; $\cos \hat{\psi} = (f - D^2/16f)/(f + D^2/16f)$.

is considered. For the case of gain maximization, the procedure is as follows:

- (1) For a given angle of main-beam pointing observation (θ_0, ϕ_0) , reflector f/D ratio and distortion profile, choose the array feed parameters N , d_e , and b .⁴
- (2) Calculate the field values $\{F_i\}$ using the Jacobi-Bessel method.
- (3) Set the array element excitations $\{a_i\}$ to the conjugate values of $\{F_i\}$ and calculate gain.

For the more general case, a performance function $f(\vec{a})$, $\vec{a} = \{a_i\}$, can be defined as the norm of the difference between the actual secondary pattern $E(\theta, \phi, \vec{a})$, and some desired secondary pattern, $E_D(\theta, \phi)$, i.e.,

$$f(\vec{a}) = \|E(\theta, \phi, \vec{a}) - E_D(\theta, \phi)\| \quad (9)$$

The statement of the problem is then

$$\text{find min } f(\vec{a}) \quad (10)$$

where some numerical search routine, such as the Rosenbrock method, is used to perform the function minimization.

V. Analysis of Focal-Plane Field Distributions for Distorted Parabolic Reflectors

An approximate expression for the focal-plane field distribution is first derived based on the scalar diffraction integral. The expression is valid for reflectors having small magnitudes of distortion and large f/D ratios. It is meant to provide some analytical insight into the effects of reflector distortion. Contour plots of the focal-plane fields, based on data from the Jacobi-Bessel method, are presented in Subsection V.C. for various cases of distortion and beam scan angle.

Using the aperture-field method, the principal component of the electric field distribution, E , in the focal plane of a large parabolic reflector can be related to the corresponding component H of the electric field in the aperture plane by a scalar equation of the form (Ref. 1)

$$E(r, \phi') = \int_0^{2\pi} \int_0^{\hat{\psi}} H(\psi, \xi) \exp [jkr \sin \xi \cos (\psi - \phi')] \times \sin \psi \, d\psi \, d\xi \quad (11)$$

where the integration is taken over the surface of the spherical cap subtended by the angle $\hat{\psi}$.

A. Undistorted Reflector

For the case of a uniform aperture distribution and a perfect reflector having $f/D > 1$, the solution to Eq. (11) has the form

$$E(r, \phi') \cong 2\pi(\hat{u})^2 \frac{J_1(kr\hat{u})}{kr\hat{u}} \quad (12)$$

where $\hat{u} = \sin \hat{\psi}$ and $J_1(x)$ is the Bessel function of first kind, first order.

B. Distorted Reflector

Small profile distortions in the reflector surface may be conveniently considered as effective phase errors, which theoretically may be projected into the aperture plane of the reflector (Ref. 9). The field distribution in the aperture plane is therefore modified by the phase error. The magnitude of the phase error, being proportional to the operating frequency, imposes an upper limit above which the reflector is ineffective as an antenna.

In what follows, models of reflector surface distortion are considered to have the form

$$\Delta z = \epsilon \rho^s \cos(L\xi) \quad (13)$$

Where ϵ is the maximum deviation in wavelengths, s is a real number, ρ is the normalized distance from the z -axis to a point on the reflector normalized to the reflector radius and L is the integer number of periodic scallops in the distorted reflector. Based on data (Ref. 10) for gravity-induced distortions as a function of pointing angle, typical of large ground-based reflectors, ϵ can vary from 0 to 0.2, s from 0.5 to 2, and L is roughly equal to 3. Random distortion errors are not considered here.

Figure 1, with all distances normalized to the reflector radius, $D/2$, in wavelengths, shows

$$u = \sin \psi = \frac{\rho}{2f/D + \rho^2/8f/D} \quad (14)$$

which for $f/D > 1$ reduces to

$$\rho \cong \left(2 \frac{f}{D}\right) u \quad (15)$$

⁴The optimum choice of the feed parameters is discussed in Section VI.

If, as discussed above, the effects of distortion are accounted for by an equivalent phase error in the aperture plane, the resulting phase error distribution, including a factor for reflector curvature as in Ref. 11, can be expressed as

$$\delta = 2\pi(1 + \cos \psi) \Delta z \quad (16)$$

If, however, the effects of reflector curvature are neglected, which is reasonable for $f/D \geq 1$, then Eq. (16) becomes

$$\delta \cong 4\pi \Delta z \quad (16a)$$

Substituting Eqs. (13) and (15) into Eq. (16a) results in

$$\delta = 4\pi \epsilon (2f/D)^s u^s \cos(L\xi) \quad (17)$$

The modified aperture field distribution then becomes

$$H(u, \xi) = \exp(j\delta) = \exp(j\epsilon' u^s \cos L\xi) \quad (18)$$

where

$$\epsilon' = 4\pi \epsilon (2f/D)^s$$

Therefore, the focal-plane field distribution, as given by Eq. (11), for the case of a distorted reflector having $f/D \geq 1$, becomes

$$E(r, \phi') = \int_0^{2\pi} \int_0^{\hat{u}} \exp[j\epsilon' u^s \cos L\xi] \cdot \exp[jkru \cos(\xi - \phi')] u du d\xi \quad (19)$$

This can be evaluated by expanding the two exponential terms in the integrand. In general, since Bessel functions of large order and small argument can be neglected, the procedure is rapidly convergent.

For the case of $s = 2$ and $L = 3$, the following result is obtained:

$$E(r, \phi') \cong 2\pi(\hat{u})^2 \frac{J_1(kr\hat{u})}{kr\hat{u}} + \frac{16\pi \epsilon' \cos(3\phi') (\hat{u})^3}{7kr} J_4(kr\hat{u}) \quad (20)$$

The first term on the right of Eq. (20) is the focal-plane field of an undistorted reflector. The second term represents a first-order approximation of the field due to distortion.

C. Contour Plots of Focal-Plane Field

Graphical insight into the effects of reflector distortion can be obtained from an examination of contour plots of the focal-plane field distribution. In Figs. 3a through 3e, such plots are shown for the case $f/D = 1.0$ and values of $\epsilon = 0, 0.12\lambda, 0.2\lambda, s = 1.0, L = 3$, and incident plane wave on-axis ($\theta_0 = 0$) and off-axis ($\theta_0 \cong 0.5 \text{ BW}$).⁵ Each of these plots is based on a triangular grid of 37 data points (see Fig. 2).

The deviation from circular symmetry and the spreading out of energy in the focal plane as a function of distortion is clearly shown by these plots. The combination of distortion and off-axis beam scan (Fig. 3e) results in particularly severe spreading of the focal-plane energy. Bearing in mind the dynamic nature of the distortion effects, these plots make it clear that it would be impossible to properly match the focal-plane fields of a distorted reflector with a conventional single-element feed.

VI. Numerical Results — Gain Maximization

In this section, quantitative information is presented about the effectiveness and feasibility of the array-feed approach, as well as optimum array-feed parameter values obtained from gain maximization calculations made using the algorithmic procedure described in Section IV. This is done for a variety of f/D ratios, beam-scan angles θ_0 , array-feed parameters (N, d_e , and b), and distortion parameters ϵ and s .

Feasibility of the array-feed approach is largely determined, from a hardware point of view, by the number and type of array-element radiators required to achieve significant gain restoration and vernier beamsteering.

The output of the algorithmic synthesis procedure is the set of array excitations that optimize performance and the resulting performance value (i.e., gain). To maximize gain with a given number of array elements N , the optimum choice of the feed parameters (d_e and b) depends on the need for greater or less granularity and/or greater or less capture area to conjugate-match the array-feed excitation to the focal-plane field distribution.

To see the relationship between gain performance and these parameters, the results of the matrix of gain calculations are presented graphically in Figs. 4a through 4e (on-axis gain loss vs d_e) for values of $N = 7, 19, 37$; $f/D = 0.4, 1.0, 1.5$; $\epsilon = 0., 0.12, 0.2$; $s = 1, 2$; and $b = 2.07$ and 2.47 . In Fig. 5, gain loss is plotted as a function of scan angle, θ , BW, for the optimum

⁵ Beamwidth, $BW \cong 1.16\lambda/D$ radians (i.e., $\cong 0.66 \text{ deg}$ for $D = 100\lambda$).

choice of d_e (taken from Figs. 4a through 4e) with $N = 7, 19, 37$ ($f/D = 1.0$). In these graphs, gain loss is referenced to the ideal maximum gain of the reflector's circular aperture (e.g., 49.94 dB for $D = 100\lambda$). It is also useful to have as a reference the gain loss results obtained with a single feed, $N = 1$, for various f/D and distortion parameter values (Table 1).

From these results it is immediately seen that: (a) the lower the f/D value and therefore the more pronounced the reflector curvature (Eq. (16)), the smaller the effects of distortion; (b) gain loss increases with increasing modulus of distortion ϵ ; and (c) gain loss is less for larger s (i.e., $s = 2$), since this corresponds to distortion concentrated at the reflector rim, while smaller s (i.e., $s = 1$) corresponds to distortion distributed more widely over the reflector surface, resulting in greater gain loss.

A. Gain Loss as a Function of the Array Parameters N, d_e, b

The results presented in Figs. 4 and 5 show that, as compared to the gain obtained with a single feed, an array feed having the proper choice of parameters can provide significant gain restoration and (for $N = 19, 37$) useful vernier beamsteering. For $N = 7$, Figs. 4a through 4c, it is seen that the value of element diameter that gives maximum on-axis gain loss is approximately that required by a single feed for the given f/D ratio, i.e.

$$\text{optimum } d_{e_{N=7}} \cong d_{e_1} \cong \sqrt{\frac{9.2}{b}} (f/D) \quad (21)$$

where d_{e_1} is given by Eq. (8b). While the amount of gain restoration is significant, there still remains some residual loss due to distortion; i.e., for the case $\epsilon = 0.12, s = 2, b = 2.07$, the gain loss is approximately 0.3 dB greater than that for $N = 1$ with no distortion (Table 1).

Also seen in Figs. 4a, b, and c for $N = 7$, the use of elements having high effective aperture, characterized by a value of $b = 2.47$, gives better on-axis gain (approximately 0.2 dB better for the case $\epsilon = 0.12, s = 2$) than elements with $b = 2.07$. This increase in gain can probably be explained by the fact that the higher value of b allows smaller array element spacing (and therefore better matching granularity) while maintaining a high effective capture area for the feed. The results presented here do not account for coupling effects, and therefore the possible advantages of using high effective aperture elements (e.g., $b = 2.47$) in an array are subject to experimental verification. In what follows, the emphasis is placed on results obtained with elements characterized by the more conservative (i.e., more realizable) value of $b = 2.07$.

As seen in Fig. 5, the optimum seven-element array will not provide continuous low-loss scanning but rather stepped scanning with beams formed on-axis and approximately 1.8 BW off-axis. This is discussed further in Subsection VI.B.

In each of the cases shown in Figs. 4a, b, and c for $N = 7$, it is seen that gain loss has an oscillatory or quasi-periodic character as a function of variable d_e : in addition to the optimum at d_{e_1} , there is a local optimum at approximately $1/3 d_{e_1}$. This can be explained heuristically as giving the number and size of identical circular elements that fill the minimum diameter d_{e_1} and that fit on a triangular grid, but that do not overlap the focal plane field null region. This explanation fits well with the results for $N = 19$ and 37, (Figs. 4d and e), where it is seen that the optimum d_e is approximately $1/3 \cdot d_{e_1}$. Therefore

$$\text{optimum } d_{e_{N=19,37}} \cong \frac{1}{3} \sqrt{\frac{9.2}{b}} (f/D) \quad (22)^6$$

From Eqs. (3), (21), and (22), it is seen that the maximum diameter of the optimum 7-element array feed is approximately 30% larger than that of the optimum 37-element array and 80% larger than that of the optimum 19-element array (Fig. 6).

For $N = 19$, the on-axis gain is hardly better than that for $N = 7$. However, for $N = 19$, very good beamsteering is obtained over a range of ± 1 BW (Fig. 5). As is the case for $N = 7$, and also for $N = 19$, the use of an element having high effective aperture characterized by a value of $b = 2.47$ does give better on-axis gain (approximately 0.2 dB better for the case $\epsilon = 0.12, s = 2$) than an element having lower effective aperture ($b = 2.07$, Fig. 4d).

For $N = 37$, the on-axis gain and the beamsteering performance is excellent over a scanning range of ± 1.5 BW (Figs. 4e and 5). In fact, over the range of ± 0.5 BW for $N = 37$, the gain with distortion ($\epsilon = 0.12, s = 2$) is equal to or better than the gain for $N = 1, 7$, or 19 with no distortion ($\epsilon = 0$). With $N = 37$, no appreciable improvement in on-axis gain is obtained by using elements having a value of $b = 2.47$.

For small values of f/D , Eq. (22) indicates that the optimum diameter is less than 0.5λ for arrays with 19 or 37 elements. In most cases, such elements would be impractically small. Therefore, in the context of this study, the use of array feeds with more than seven elements for reflectors with small f/D values (e.g., 0.4) would not be practical.

⁶For $N = 19$, the numerical results indicate that the optimum d_e is approximately 10% larger than that given by Eq. (22).

Finally, in Fig. 7, the secondary patterns of a distorted reflector with $f/D = 1$, $\epsilon = 0.12$, and $s = 2$ are shown for feeds with (a) $N = 1$ ($d_e = 2.1$) and (b) $N = 37$ ($d_e = 0.71$). Note that the array feed ($N = 37$) has produced a secondary pattern that is reasonably symmetric despite the asymmetric reflector distortions.

B. Beamsteering

To deal with the question of beamsteering, a simple analysis is made based on the reflector/array feed geometry. For large apertures, the scan angle θ_s is approximately

$$\theta_s \approx \frac{r}{f} BDF \quad (23)$$

where r is the radial distance of the feed away from the focal point origin, and BDF is the beam deviation factor, which is $\cong 1$ for $f/D \geq 1$. The number of beamwidths of scan for a scan angle of θ_s is given by

$$\frac{\theta_s}{BW} \cong \frac{D}{1.16\lambda} \cdot \frac{r}{f} \cdot BDF \quad (24)$$

where the secondary pattern beamwidth, $BW \cong 1.16\lambda/D$.

Now, the set of elements that comprise the array generates a set of corresponding beams in the far field. To achieve continuous, low-loss scan, the far-field beam crossovers should not be lower than their 3-dB points. To achieve this, it is necessary that

$$\frac{\theta_s}{BW} \leq 1 \quad (25)$$

For $r = d_e$ (the radial distance to the first ring of elements in the feed array), Eqs. (24) and (25) imply that

$$d_e \leq \frac{1.16\lambda}{BDF} (f/D) \quad (26)$$

The restrictions imposed by Eq. (26) on d_e for continuous, low-loss beamsteering performance may not, in all cases, be consistent with the requirements for optimum on-axis gain correction. For example, with $N = 7$ and $f/D = 1$, the on-axis gain is optimized with $d_e \cong 2.1\lambda$ [Fig. 4b and Eq. (21)]. This value of d_e does not satisfy Eq. (26). By Eq. (23), the scan angle θ_s for an element located at 2.1λ is approximately 1.8 BW and not ≤ 1 BW as required for continuous, low-loss beamsteering. The array feed in this example gives good “stepped” beamsteering but not continuous beamsteering (e.g., $G(0 \text{ BW}) \cong -0.8 \text{ dB}$ and $G(1.8 \text{ BW}) \cong -0.8 \text{ dB}$ but $G(1 \text{ BW}) \cong -7.0 \text{ dB}$ (see Fig. 5). On the other hand, for $N = 37$, the optimum value of d_e to maximize on-axis gain is $\cong 0.71\lambda$ [Fig. 4e or Eq. (22)], which does satisfy Eq. (26), giving excellent, continuous, low-loss beamsteering performance (Fig. 5).

VII. Conclusions

This study has shown that a planar array feed has excellent potential as a solution to paraboloidal reflector distortion problems and beamsteering requirements. The numerical results obtained show that, for the range of distortion models considered, good on-axis gain restoration can be achieved with as few as seven elements. For beamsteering to ± 1 BW, 19 elements are required. For arrays with either 7 or 19 elements, high effective aperture elements (e.g., $b = 2.47$) give higher system gain than elements having lower effective apertures (e.g., $b = 2.07$). With 37 elements, excellent gain and beamsteering performance to ± 1.5 BW are obtained independently of the assumed effective aperture of the array element. Simple “rules of thumb” for the design of the planar array feed configuration have been presented.

References

1. Rudge, A. W., and Davies, D. E. N., "Electronically Controllable Primary Feed for Profile Error Compensation of Large Parabolic Reflectors," *Proc. IEEE (Brit.)*, Vol. 117, No. 2, pp. 351-358, February 1970.
2. Amitay, N., and Zucker, H., "Compensation of Spherical Reflector Aberrations by Planar Array Feeds," *IEEE Trans.*, Vol. AP-20, No. 1, pp. 49-56, January 1972.
3. Imbriale, W. A., Galindo-Israel, V., Rahmat-Samii, Y., and Bruce, R. L., "Improved Wide-Angle Scan Using a Mini-Max Optimization Technique," *Proceedings of the URSI Meeting*, Houston, Texas, May 1983.
4. Blank, S. J., and Imbriale, W. A., "Array Feed Synthesis for Correction of Reflector Distortion and Vernier Beamsteering," *Proceedings of the International Radio Science Union (URSI) Meeting*, Boulder, Colorado, January 1983.
5. Rahmat-Samii, Y., and Galindo-Israel, V., "Shaped Reflector Antenna Analysis using the Jacobi-Bessel Series," *IEEE Trans.*, Vol. AP-28, pp. 425-435, July 1980.
6. Collin, R. E., and Zucker, F. J., *Antenna Theory*, McGraw-Hill, New York, New York, 1969.
7. Rahmat-Samii, Y., Cramer, P., Woo, K., Lee, S. W., "Realizable Feed Element Patterns for Multibeam Reflector Antenna Analysis," *IEEE Trans.*, Vol. AP-29, No. 6, pp. 961-963, November 1981.
8. Wilde, D. J., and Beightler, C. S., *Foundations of Optimization*, Prentice-Hall, Inc., 1967.
9. Silver, S., *Microwave Antenna Theory and Design*, McGraw-Hill, New York, New York, 1949.
10. Katow, M. S., *Structural Technology for Large Radio and Radar Telescope Systems*, pp. 185-280, J. W. Mar and H. Liebowitz, Eds., MIT Press, Cambridge, Massachusetts, 1969.
11. Imbriale, W. A., and Rusch, W. V. T., "Scalar Analysis of Distorted Umbrella Reflector," *IEEE Trans.*, Vol. AP-22, pp. 112-114, January 1974.

Table 1. Gain loss with a single feed, $N = 1$ ($b = 2.07$)

f/D	d_{e1}, λ	ϵ, λ	Gain Loss, dB	
			$s = 2.0$	$s = 1.0$
0.4	0.9	0	-0.84	-0.84
		0.12	-1.56	-2.07
		0.2	-2.83	-5.28
1.0	2.2	0	-0.89	-0.89
		0.12	-1.95	-2.63
		0.2	-3.79	-6.72
1.5	3.2	0	-0.90	-0.90
		0.12	-2.04	-2.74
		0.2	-4.00	-7.03

d_{e1} is chosen to be slightly larger than is optimum when there is no distortion ($\epsilon = 0$), to give better gain with distortion.

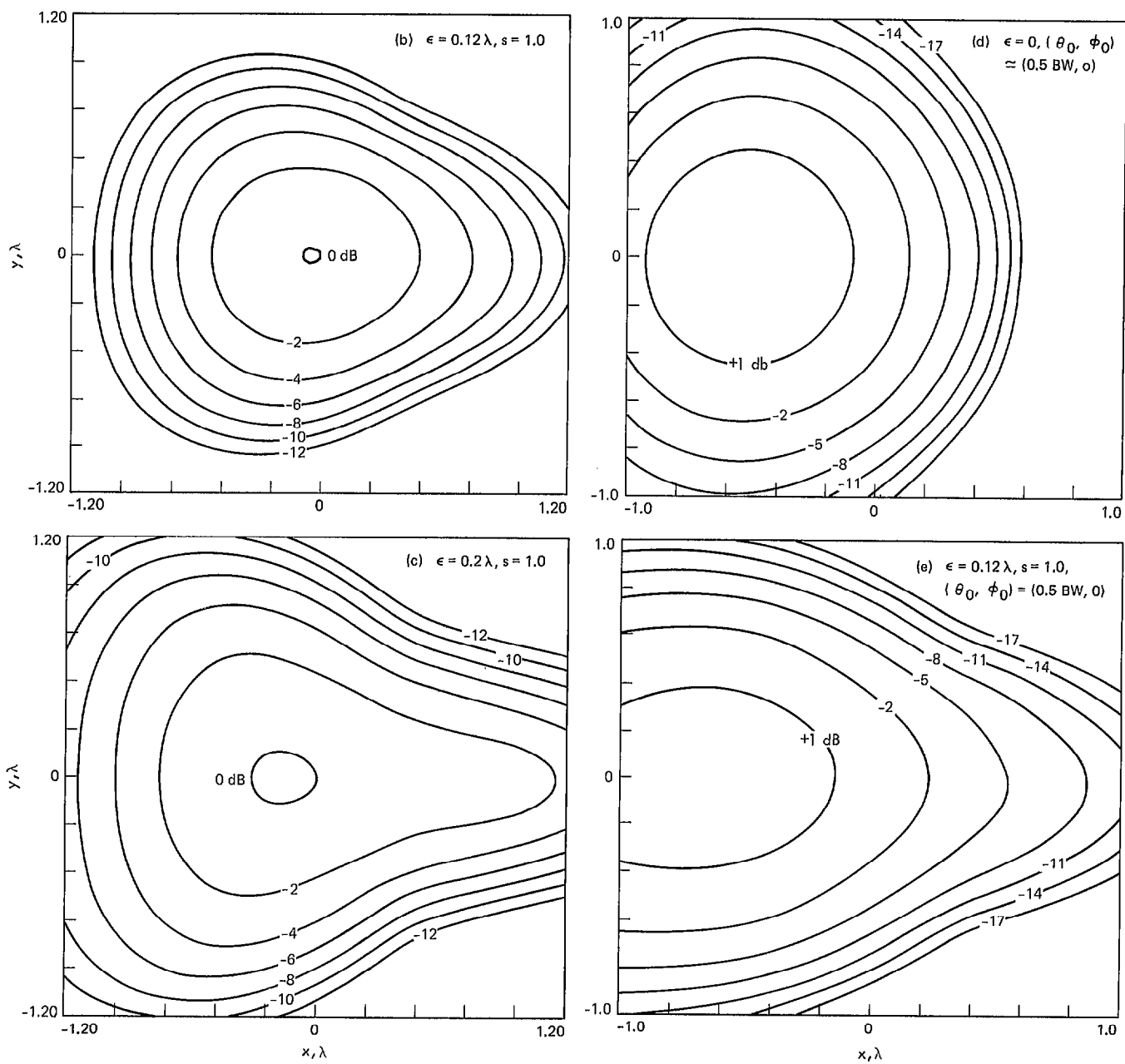


Fig. 3 (contd)

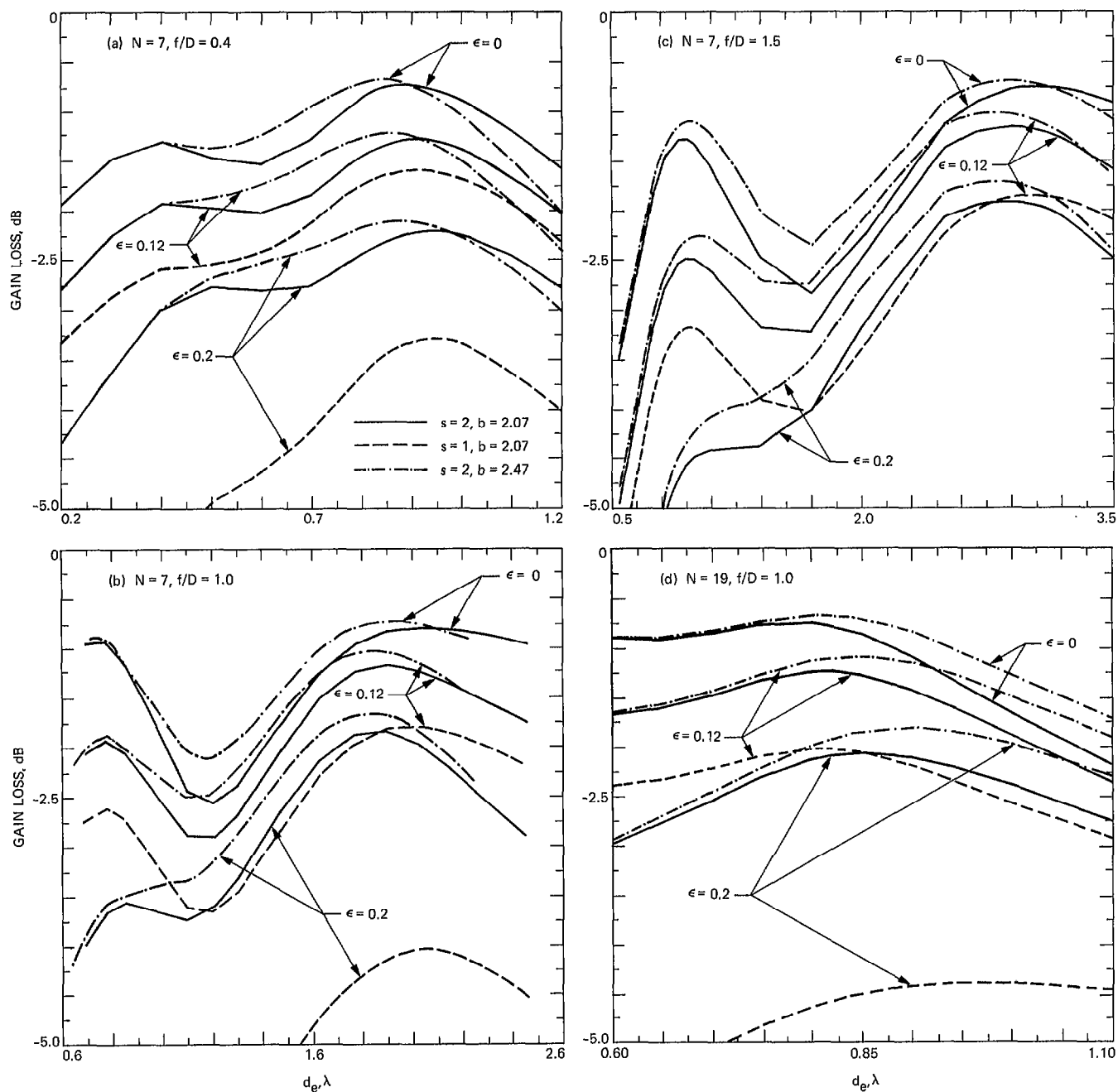


Fig. 4. On-axis gain loss as a function of element spacing

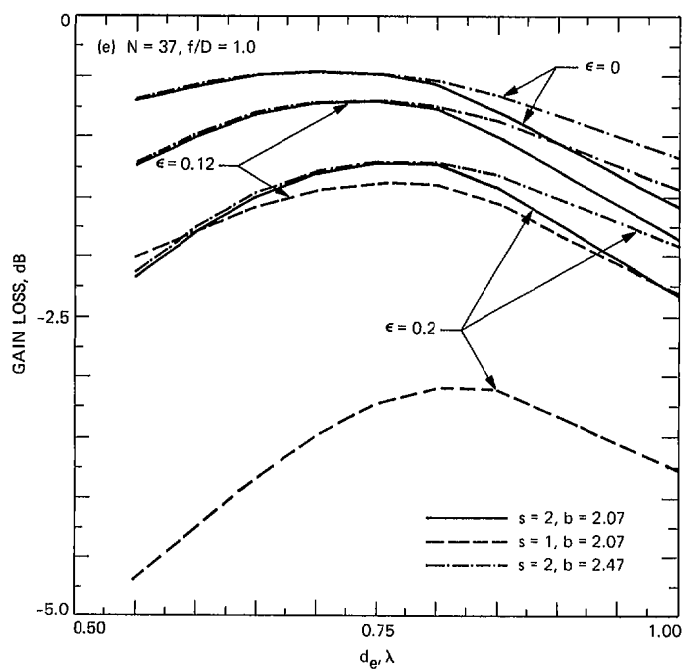


Fig. 4 (contd)

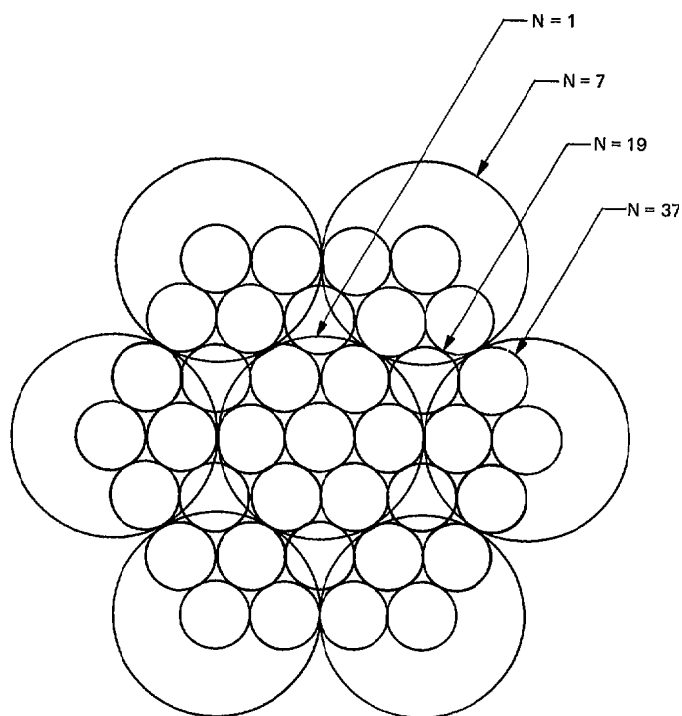


Fig. 6. Optimum array feed configurations for $N = 1, 7, 19$, and 37 elements

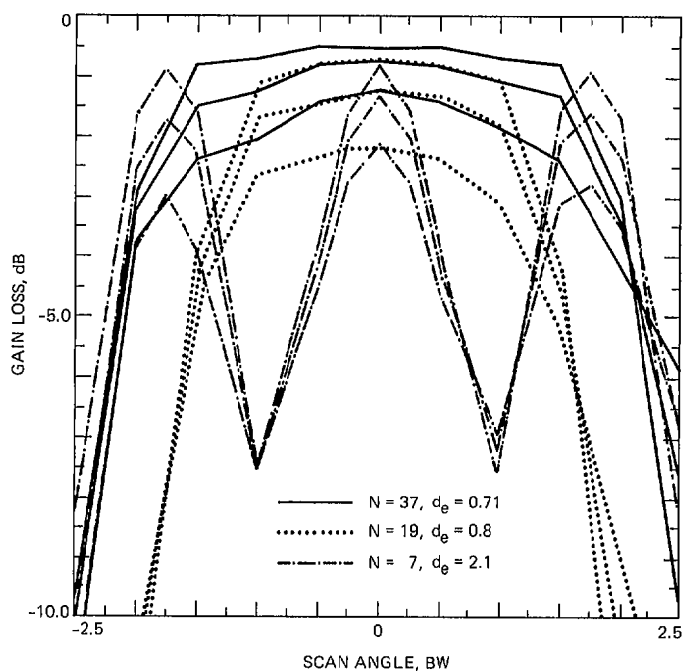


Fig. 5. Gain loss as a function of scan angle ($f/D = 1.0$, $s = 2$, $\epsilon = 0, 0.12, 0.2$)

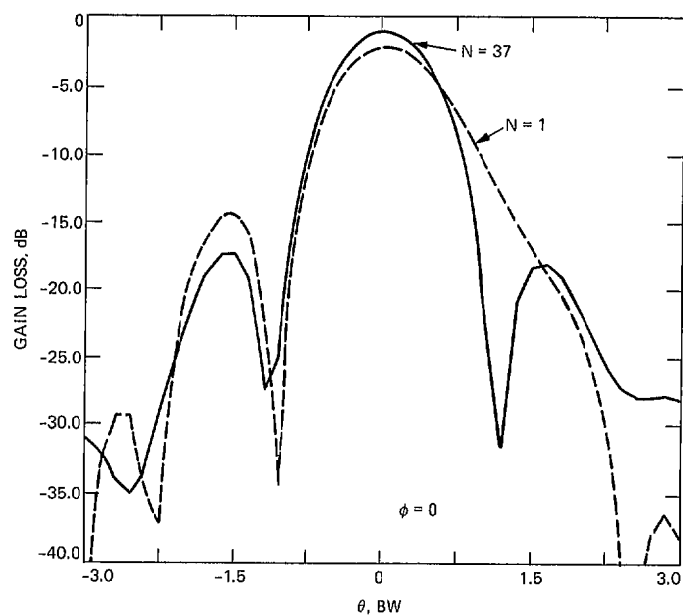


Fig. 7. Secondary patterns of distorted reflector ($f/D = 1.0$, $\epsilon = 0.12\lambda$, $s = 2.0$ for $N = 1$, $d_e = 2.1$, and $N = 37$, $d_e = 0.71$)